

CIPHERPRUNE: EFFICIENT AND SCALABLE PRIVATE TRANSFORMER INFERENCE

Anonymous authors

Paper under double-blind review

ABSTRACT

Private Transformer inference using cryptographic protocols offers promising solutions for privacy-preserving machine learning; however, it still faces significant runtime overhead (efficiency issues) and challenges in handling long-token inputs (scalability issues). We observe that the Transformer’s operational complexity scales quadratically with the number of input tokens, making it essential to reduce the input token length. Notably, each token varies in importance, and many inputs contain redundant tokens. Additionally, prior private inference methods that rely on high-degree polynomial approximations for non-linear activations are computationally expensive. Therefore, reducing the polynomial degree for less important tokens can significantly accelerate private inference. Building on these observations, we propose *CipherPrune*, an efficient and scalable private inference framework that includes a secure encrypted token pruning protocol, a polynomial reduction protocol, and corresponding Transformer network optimizations. At the protocol level, encrypted token pruning adaptively removes unimportant tokens from encrypted inputs in a progressive, layer-wise manner. Additionally, encrypted polynomial reduction assigns lower-degree polynomials to less important tokens after pruning, enhancing efficiency without decryption. At the network level, we introduce protocol-aware network optimization via a gradient-based search to maximize pruning thresholds and polynomial reduction conditions while maintaining the desired accuracy. Our experiments demonstrate that *CipherPrune* reduces the execution overhead of private Transformer inference by approximately $6.1\times$ for 128-token inputs and $10.6\times$ for 512-token inputs, compared to previous methods, **with only a marginal drop in accuracy**. The code is publicly available at <https://anonymous.4open.science/r/CipherPrune-8AEC>.

1 INTRODUCTION

Transformers (Vaswani et al., 2017) have become the predominant approach for tackling a wide range of machine learning tasks, spanning Natural Language Processing (NLP) and Computer Vision (CV) domains. Notably, Transformer-as-a-Service (TaaS) (Radford et al., 2018) has emerged as an effective means for average users to harness the capabilities of sophisticated and accurate Transformers deployed on cloud servers. Privacy has become a major concern, driving a growing demand for privacy-preserving TaaS solutions (Zheng et al., 2023; Hao et al., 2022; Zeng et al., 2023).

Homomorphic Encryption (HE)(Gentry, 2009) is a promising secure computing technology that protects data privacy by enabling computations on encrypted data without decryption. However, applying HE continuously for deep computation tasks often results in prohibitively high latency. To address this, hybrid HE/Multi-party Computation (MPC)-based techniques(Chen et al., 2022; Zheng et al., 2023; Hao et al., 2022; Zeng et al., 2023; Zhang et al., 2023; Lu et al., 2025; Pang et al., 2024; Xu et al., 2024) have been widely adopted for private Transformer inference, as illustrated in Figure 1 (a). This hybrid approach achieves state-of-the-art performance by using HE for linear operations and MPC for non-linear operations.

Unfortunately, prior private Transformer inferences (Lu et al., 2025; Pang et al., 2024) still suffer from significant latency and poor scalability over long-token inputs. Specifically, as Figure 1 (b) shows, the prior private inference process for a GPT2 Transformer (Pang et al., 2024) with 128 input tokens extends to ~ 10 minutes. It necessitates the exchange of over 60 gigabytes of data between

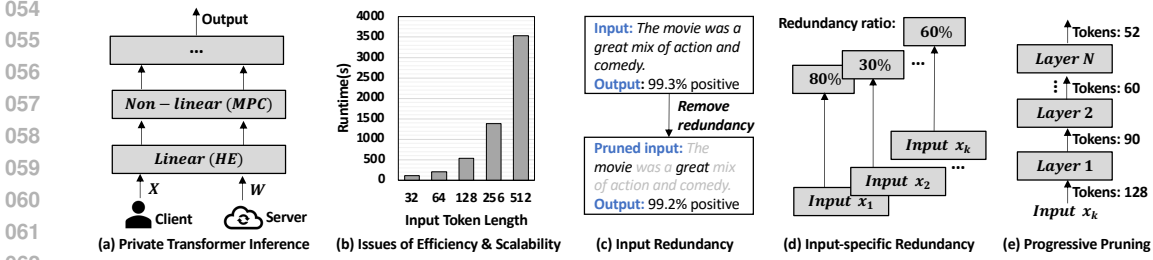


Figure 1: (a) An illustration of HE/MPC-based private inference. (b) The high-latency and scalable challenge of private Transformer models over lengthy inputs. (c) An example of redundant input in sentiment analysis tasks. (d) Demonstration of varying levels of redundancy across different inputs. (e) An example showcasing progressive redundancy pruning.

the server and the client. Furthermore, as the token length increases, the runtime overhead grows super-linearly, indicating poor scalability. This is primarily because the operational complexity of Transformers (Vaswani et al., 2017; Kim et al., 2022) scales quadratically with the number of input tokens. Reducing the number of input tokens without compromising accuracy is essential.

We observe that most inputs contain redundant words/tokens, with varying levels of redundancy across different inputs. As illustrated in Figure 1(c), in a sentiment analysis task, an input that retains only the tokens *movie* and *great* while removing almost all others still maintains inference confidence and accuracy. We refer to such tokens that can be removed without significantly impacting accuracy as *redundancy*. Meanwhile, the different inputs have various levels of redundancy (Wang et al., 2021; Kim et al., 2022). Figure 1 (d) illustrates that some inputs exhibit greater redundancy, while others have less, with this variation being particularly evident across different tasks. Classification tasks typically have more redundancy compared to sequence-to-sequence tasks (Fu et al., 2024). To effectively prune more tokens from longer inputs and potentially reduce the Transformer’s quadratic complexity to linear, pruning should be done progressively—that is, tokens should be pruned layer by layer over multiple stages, as illustrated in Figure 1 (e), rather than performing a one-time pruning at the first layer (Wang et al., 2021; Kim et al., 2022). Another key observation is that previous private Transformer inference methods, whether relying on precise non-linear activations (Hao et al., 2022) or using large-degree polynomial approximations (Lu et al., 2025; Pang et al., 2024) for these activations, continue to suffer from significant execution overhead for non-linear operations. Therefore, replacing non-linear activations or high-degree polynomials with lower-degree polynomials can be beneficial. As shown in Figure 2 , a degree- d polynomial activation for tokens (Figure 2(a)) can be reduced to a degree- d_i polynomial (Figure 2(b)), where $d_i \leq d$.

Adopting existing plaintext-level pruning techniques (*PlainPrune*) (Wang et al., 2021; Kim et al., 2022) to accelerate private Transformer inferences presents a formidable challenge. The primary reason is that the tokens are encrypted, and we need to calculate token importance scores layer by layer for specific encrypted inputs. This requires redesigning a new encrypted token pruning protocol. Meanwhile, the polynomial reduction in the encrypted domain poses a similar challenge, and we need to design an encrypted polynomial reduction protocol for efficient private activation. Also, at the network level, we need to learn the pruning and polynomial reduction thresholds while maximizing *efficiency*, ensuring *privacy*, and maintaining the desired level of *accuracy*.

To address these challenges, we introduce CipherPrune, a scalable and efficient framework for private inference that incorporates a secure encrypted token pruning protocol, a polynomial reduction protocol, and tailored Transformer network optimizations. At the protocol level, CipherPrune adaptively prunes unimportant tokens from encrypted inputs in a progressive, layer-by-layer manner. It also applies encrypted polynomial reduction by assigning lower-degree polynomials to less important tokens post-pruning, thereby improving efficiency without requiring decryption. At the network level, we implement protocol-aware optimization using a gradient-based search, aiming to maximize pruning thresholds and polynomial reduction conditions while preserving the required accuracy. Our experiments show that CipherPrune reduces the execution overhead of private Transformer inference by about $6.1 \times$ for 128-token inputs and $10.6 \times$ for 512-token inputs compared to prior method (Pang et al., 2024), **with only a marginal drop in accuracy**.

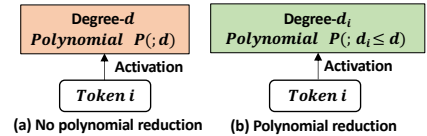


Figure 2: Polynomial Reduction.

2 PRELIMINARIES

Attention-based Transformers. Attention mechanisms underpin the superior performance of Transformers, which can effectively capture long-range dependencies in the input token sequence and model contextual information. The Transformer (Devlin et al., 2018) consists of multiple encoder and decoder layers, both of which share the similar structure. A basic transformer encoder layer consists of two major computation blocks: a Multi-head Self-attention (MHA) module and a Feed Forward (FFN) module, each with residual connections around and followed by a Layer Normalization (LN) module. Given an input token sequence $x \in \mathbb{R}^{n \times D}$, where n is the number of tokens and D is the token embedding dimension, the attention is computed as: $Attention(Q, K, V) = SoftMax(QK^T / \sqrt{d_h})V$. The matrices $Q, K, V \in \mathbb{R}^{n \times d_h}$ are computed by multiplying input x with three weight matrices $W_q, W_k, W_v \in \mathbb{R}^{D \times d_h}$, where d_h is the head dimension.

Token Pruning in Transformers. To reduce the computational overhead of plaintext Transformers, a range of strategies including efficient architecture design, knowledge distillation, quantization, and both model and token pruning have been developed. Among these, token pruning (Goyal et al., 2020; Kim & Cho, 2020; Wang et al., 2021) stands out for its ability to dynamically reduce token complexity, enhancing efficiency for scalable input lengths. Online token pruning progressively eliminates nonessential input tokens during inference, with recent techniques like learning-based token pruning assigning tunable thresholds to each Transformer layer. These thresholds are fine-tuned during training to maximize the removal of tokens from the sequence.

Given the attention map $Att = SoftMax(QK^T / \sqrt{d}) \in \mathbb{R}^{n \times n}$, the importance score $S \in \mathbb{R}^n$ of n tokens $x_i \in \mathbb{R}^D$ in the input sequence can be computed as: $S[i] = \frac{1}{H} \frac{1}{n} \sum_{h=0}^{H-1} \sum_{j=0}^{n-1} Att^h[j, i]$ (1) where H is the number of attention heads and Att^h is the attention map in the h -th head. Importance score S is essentially computed by accumulating attention scores vertically, which indicates the importance of a token across all heads in one Transformer layer.

Cryptographic Primitives. Our protocol uses multiple cryptographic primitives including Additive Secret Sharing (ASS), Homomorphic Encryption (HE), and Oblivious Transfer (OT).

- **ASS.** We employ a 2-out-of-2 ASS scheme (Cramer et al., 2015) operating over the ring \mathbb{Z}_ℓ , where ℓ is the bitwidth of the input x . ASS partitions x into two distinct random shares $\langle x \rangle_0, \langle x \rangle_1$, where $x = \langle x \rangle_0 + \langle x \rangle_1 \bmod \mathbb{Z}_\ell$. The parties, P_0 and P_1 , respectively hold $\langle x \rangle_0, \langle x \rangle_1$. Importantly, it is guaranteed that neither P_0 nor P_1 can discern the actual value of x (Cramer et al., 2015). ASS lends itself to linear operations, i.e., addition and constant multiplication, without communications.
- **HE.** We leverage the BFV scheme (Brakerski, 2012; Fan & Vercauteren, 2012), a leveled HE scheme, to facilitate linear operations on ciphertexts. The HE scheme has 4 functions: KeyGen, Enc, Dec, and Eval. KeyGen generates a public key pk and a secret key sk . Enc encrypts a message m with the public key pk to yield a ciphertext c . Dec, with the secret key sk and ciphertext c as inputs, decrypts the ciphertext to recover the message m . Finally, Eval, when given the public key pk , two ciphertexts c_1 and c_2 encrypting messages m_1 and m_2 , along with a linear function \mathcal{F} , produces a new ciphertext c' encrypting the result of $\mathcal{F}(m_1, m_2)$.
- **OT.** We use OT for non-linear operations (Rathee et al., 2020; 2021) in a network model. Specifically, we employ 1-out-of-2 correlated OT (Asharov et al., 2013) (2-COT $_\ell$) and 1-out-of- k (Kolesnikov & Kumaresan, 2013) (k -OT $_\ell$). In 2-COT $_\ell$, the protocol takes as inputs the sender’s correlation $x \in \mathbb{Z}_\ell$ and receiver’s bit choice $i \in \{0, 1\}$. It then produces a random element $r \in \mathbb{Z}_\ell$ for the sender and $r + i \cdot x$ for the receiver. In k -OT $_\ell$, the sender possesses k messages m_0, \dots, m_{k-1} and the receiver holds an index $i \in [k]$. The protocol ensures the receiver learns x_i as the output without learning any information about x_j , where $j \in [k]$ and $j \neq i$, while the sender learns nothing about the receiver’s choice i .

CipherPrune reuses partial existing protocols detailed in Appendix B.

Prior Private Transformer Inference. In response to the success of Transformers and the need to safeguard data privacy, various private Transformer Inferences (Chen et al., 2022; Zheng et al., 2023; Hao et al., 2022; Li et al., 2022; Lu et al., 2025; Hou et al., 2023; Luo et al., 2024; Pang et al., 2024) are proposed. To efficiently run private Transformer inferences, multiple cryptographic primitives are used in a popular hybrid HE/MPC method IRON (Hao et al., 2022), i.e., in a Transformer, HE and SS are used for linear layers, and SS and OT are adopted for nonlinear layers. IRON and BumbleBee (Lu et al., 2025) focus on optimizing linear general matrix multiplications; SecFormer (Luo et al., 2024)

improves non-linear operations, such as the exponential function, through polynomial approximation. BOLT (Pang et al., 2024) introduces the baby-step giant-step (BSGS) algorithm to reduce the number of HE rotations, proposes a word elimination (W.E.) technique, and uses polynomial approximation for non-linear operations, ultimately achieving state-of-the-art (SOTA) performance. It’s worth noting that the W.E. technique in BOLT is not input-specific, as it uniformly prunes half the tokens regardless of the input or task. This approach may fail to remove all redundancy when it exceeds half of the tokens and can harm accuracy when redundancy is less than half. Additionally, since W.E. performs one-time pruning at the first layer rather than progressive, layer-by-layer pruning, it is less effective at reducing tokens for longer inputs. Moreover, BOLT’s W.E. protocol is computationally expensive due to its reliance on sorting, whereas our method achieves lower asymptotic complexity and faster concrete runtime. Specifically, the state-of-the-art BOLT still faces efficiency and scalability challenges with long-token inputs. For example, one private inference with a GPT2-Base model can take ~ 10 minutes for 128-token inputs and ~ 1 hour for 512-token inputs, requiring data exchanges of more than 60GB and 200GB, respectively. Besides the hybrid HE/MPC methods, a line of works has explored performing private Transformer inference with only HE (Zimerman et al., 2023; Zhang et al., 2024). We leave a more detailed review of related works in Appendix G.

Threat Model and Security Guarantee. CipherPrune operates in a common private inference scenario where server P_0 owns a proprietary Transformer-based model \mathcal{M} with private weights w , and client P_1 possesses private input data x . We assume the server and client are semi-honest, i.e., the server and client follow the designed protocols but are curious and attempt to learn extra information (e.g., x or w). This setting is practical, as the server is incentivized to follow protocols and provide high-quality services for monetary gain, while the client is motivated to adhere to the protocol to receive those services. Consequently, this semi-honest setting is commonly adopted in existing works (Rathee et al., 2020; Huang et al., 2022; Hao et al., 2022; Lu et al., 2025; Pang et al., 2024). In this semi-honest setting, our protocols prevent the server from learning the client’s data and the inference result; meanwhile, these protocols also block the client from accessing the model’s parameters. In our protocols, we assume that both the server and client are aware of the number of pruned tokens. We argue that this information does not compromise the client’s data or inference results, nor does it enable the client to access the model’s weight parameters. Attacks that deviate from the semi-honest setting are beyond the scope of this work.

3 CIPHERPRUNE FRAMEWORK

3.1 MOTIVATION

Although plaintext pruning methods (Goyal et al., 2020; Kim & Cho, 2020; Wang et al., 2021) enable efficient and scalable inference for standard plaintext-domain Transformers, integrating these techniques into private Transformers remains challenging. Additionally, encrypted polynomial reduction and its joint optimization with token pruning remain largely unexplored.

Challenge 1: Lacking protocols for input-specific, progressive encrypted token pruning and encrypted polynomial reduction. The efficiency and scalability of plaintext pruning methods (Goyal et al., 2020; Kim & Cho, 2020; Wang et al., 2021) rely on two important features: (1) Input-specific pruning: This involves assigning an adaptive pruning ratio based on the dynamic importance of each input, as different inputs exhibit varying levels of redundancy. A fixed pruning ratio applied universally can result in suboptimal pruning or excessive pruning, leading to catastrophic accuracy loss. (2) Progressive pruning: This approach prunes tokens layer by layer, rather than performing a one-time early-layer pruning. Early pruning may fail to correctly identify redundant tokens, resulting in suboptimal or incorrect pruning. As mentioned earlier, prior W.E. in BOLT (Pang et al., 2024) is not input-specific or progressive. Furthermore, there is an absence of an encrypted protocol for polynomial production aimed at reducing the overhead of non-linear approximations.

Challenge 2: Lacking network optimization to support joint token pruning and polynomial reduction. In plaintext-domain token pruning (Goyal et al., 2020; Kim & Cho, 2020; Wang et al., 2021), there is no strong motivation to use polynomials to approximate non-linear activations, as these operations are straightforward and inexpensive to compute. However, in the ciphertext domain, large-degree polynomials are employed to approximate non-linear functions for both efficiency and accuracy. We observed that polynomials of varying degrees can be assigned to different tokens in the encrypted domain based on their importance scores, which can also be optimized alongside token

pruning. For instance, joint optimization of polynomial reduction and token pruning is essential, and network optimization involves searching for the optimal pruning and reduction thresholds.

CipherPrune Overview. In this paper, we introduce CipherPrune for an efficient and scalable private Transformer inference. Figure 3 shows the overview of CipherPrune. We first propose encrypted token pruning for both linear and non-linear activations in Section 3.2. Then, we develop an encrypted polynomial reduction for efficient non-linear operations in Section 3.3. We also introduce a network optimization for the joint optimization of token pruning and polynomial reduction in Section 3.4.

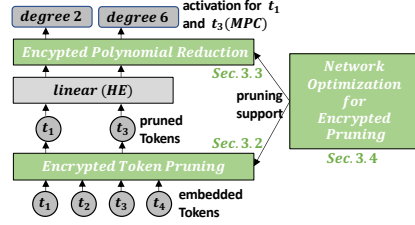


Figure 3: Overview of CipherPrune.

Figure 4 shows the workflow of a private Transformer inference implementation with our CipherPrune. During the private inference, \Uparrow the client’s input is encrypted and multiplied with the embedding matrix in the server by the Π_{MatMul} protocol. Then the result will be added to the positional encoding. The server performs the private attention computations, including linear projection via Π_{MatMul} and non-linear attention map via $\Pi_{SoftMax}$, respectively. After obtaining the tokens and attention maps, our proposed encrypted token pruning method is performed to calculate token importance scores and compare these scores with the pruning threshold θ and reduction threshold β to decide which tokens will be pruned or reduced in a privacy-preserving manner. The pruned tokens are discarded such that the following layers will have fewer operations. Low-degree polynomials are used to compute the GELU and SoftMax functions on reduced tokens. ¹ Layernorm and Feedforward operations will be executed via the prior protocols, $\Pi_{LayerNorm}$, Π_{MatMul} and Π_{GeLU} . We detail our proposed encrypted token pruning method in the subsequent subsections.

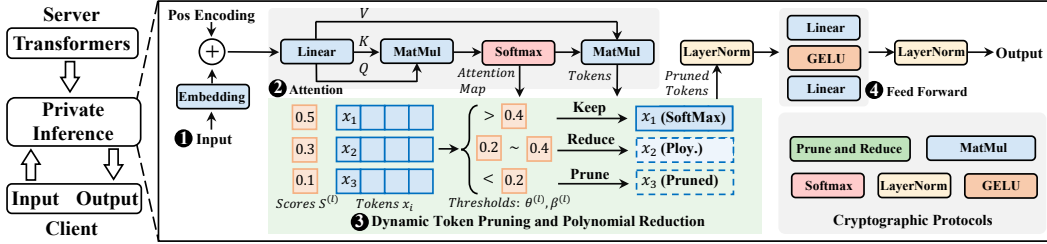


Figure 4: The workflow of a private Transformer inference with CipherPrune.

3.2 ENCRYPTED TOKEN PRUNING

Pruning protocol Π_{prune} . In private inference, confidentially pruning tokens presents a challenge, as the server and client must share attention maps and inputs without accessing their actual values. As depicted in Figure 5, during inference, attention maps are protected using ASS, with each party only able to view their respective shares.

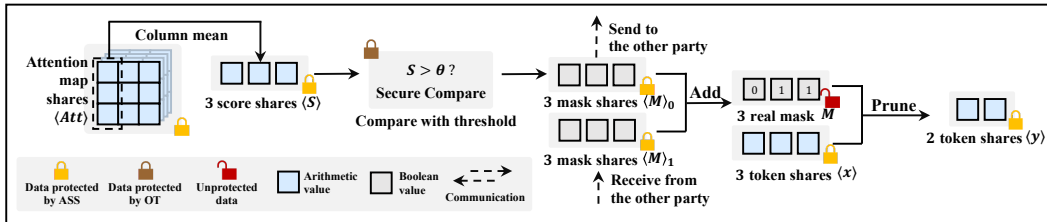


Figure 5: Illustration of mask generation and token pruning in Π_{prune} with a non-sharing mask.

Specifically, the proposed secure token pruning protocol takes the secret-shared attention maps $\langle Att \rangle^h$ and tokens $\langle x \rangle$ as inputs, and outputs the pruned tokens $\langle y \rangle$ in a secret-sharing format. The secret shares are held by server P_0 and client P_1 , respectively. First, P_0 and P_1 compute the importance score on their local secret shares, respectively. As depicted in Equation 1, the computation of the importance score involves only addition and constant multiplication, which can be performed efficiently via ASS. After P_0 and P_1 acquire their respective shares of the importance score $\langle S \rangle$,

they initiate a comparison protocol Π_{CMP} . This protocol contrasts the importance score against the threshold θ learned offline, enabling them to determine the shares of the resultant mask $\langle M \rangle$, where M is 1 if $S > \theta$, otherwise 0.

Possessing the shares $\langle M \rangle$ without access to their real values prevents the direct pruning of tokens $\langle x \rangle$. A feasible solution involves reconstructing the non-shared mask, allowing both parties to independently prune their shares of the input sequence of n tokens $\langle x \rangle$. This process then enables them to obtain the shares of the pruned output sequence of m tokens $\langle y \rangle$. Appendix A, Figure 13 includes a more detailed and formal definition of Π_{prune} .

The overhead for our secure token pruning protocol is minimal. The importance score can be computed directly on shares, taking only 0.1 ms per attention module. This is efficient even for large models like BERT-Large, which has 24 heads per layer. Additionally, our protocol only requires n invocations of the comparison protocol Π_{CMP} , each consistently completed within 5 ms, independent of the number of heads or embedding dimension. Thus, the total time complexity of our pruning protocol Π_{prune} is linear, $O(n)$, based on the input token sequence length n .

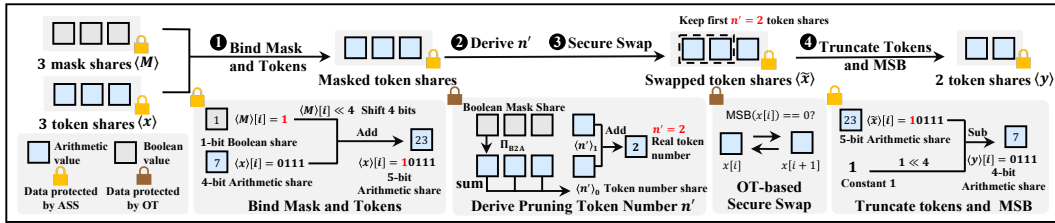


Figure 6: Example of token pruning with a protected mask.

Pruning Mask Protocol Π_{mask} . To further safeguard the privacy of the binary pruning mask M , specifically to protect the locations of pruned tokens, we design an additional Pruning Mask Protocol, Π_{mask} . The goal is to ensure that both parties, P_0 and P_1 , can obtain the pruned token sequence without knowing which specific tokens were pruned. One key observation is that the number of tokens after pruning, n' , can be safely disclosed, as it is essential for subsequent processing and is not typically associated with significant security risks like adversarial attacks (Cui et al., 2021). Knowing n' is crucial because token pruning involves relocating the less-important $m = n - n'$ tokens to the end of the token sequence while maintaining the order of the remaining n' tokens. After this rearrangement, one can simply discard the m ASS tokens at the end of the token list.

Figure 6 shows the secure mask protocol Π_{mask} that is used to ensure the mask privacy in Π_{prune} . The protocol takes secret-shared token sequence $\langle x \rangle$ and mask $\langle M \rangle$ as inputs, and generates the pruned tokens $\langle y \rangle$. **¶ Bind Mask and Tokens.** To swap tokens, their corresponding links with the mask will be disrupted. To preserve these links, there are two methods: one is to swap the masks and tokens respectively and simultaneously; the other is to bind the mask and tokens together so that they can be swapped as a unit. We adopt the second method, as binding the mask and tokens together proves more efficient than managing separate swaps for the mask and tokens. The bounded tokens $\langle \bar{x} \rangle$ can be obtained via left-shifting $\langle M \rangle$ by f bits and adding to $\langle x \rangle$, where f is the bit width of a token in x . Figure 6 illustrates using $f = 4$ as an example; however, in practice, f can be flexibly adjusted. **· Derive Pruning Token Number n' .** We found that n' can be obtained by securely counting the number of 1s in M , which does not reveal the locations of 1s in M . Specifically, to determine n' , both P_0 and P_1 first convert their boolean mask shares $\langle M \rangle$ into a fixed-point format using Π_{B2A} . Each party then locally computes the sum of the arithmetic mask using ASS, yielding $\langle n' \rangle$. Finally, P_0 and P_1 obtain n' by summing their respective shares, $\langle n' \rangle_0$ and $\langle n' \rangle_1$.

$$Swap(\bar{x}[i], \bar{x}[i+1]) = \begin{cases} b \cdot \bar{x}[i] + (1-b) \cdot \bar{x}[i+1], \\ b \cdot \bar{x}[i+1] + (1-b) \cdot \bar{x}[i]. \end{cases} \quad (2)$$

Secure Swap. This step aims to enable P_0 and P_1 to iteratively move m tokens to the end of the token sequence via OT-based oblivious swap defined in Equation 2. In each iteration, P_0 and P_1 perform an oblivious swap through the token sequence. To privately swap two tokens $\bar{x}[i]$ and $\bar{x}[i+1]$, they first extract the MSB b from the bounded token $\bar{x}[i]$ and perform four OT-based multiplications.

1 Truncate Tokens and MSB. P_0 and P_1 can truncate the swapped token sequence $\langle \bar{x} \rangle$ and remove

the MSB respectively to obtain the pruned token sequence. Figure 14 in the Appendix A details more about the mask protection protocol.

Analysis. The complexity of the proposed Π_{mask} mainly depends on the number of oblivious swaps. To prune m tokens out of n input tokens, $O(mn)$ swaps are needed. Since token pruning is performed progressively, only a small number of tokens are pruned at each layer, which makes Π_{mask} efficient during runtime. Specifically, for a BERT-Base model with 128 input tokens, the pruning protocol only takes $\sim 0.9s$ on average in each layer.

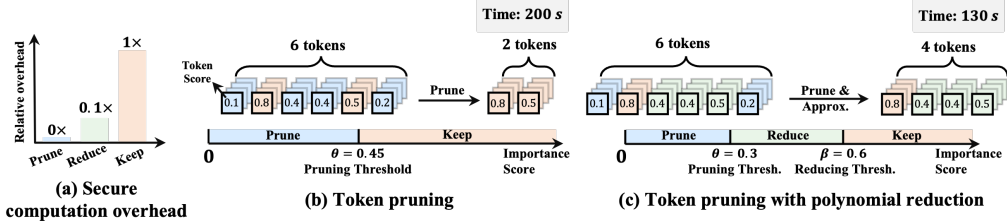


Figure 7: Comparison of token pruning-only method and pruning with polynomial reduction.

3.3 ENCRYPTED POLYNOMIAL REDUCTION

After pruning, retained tokens still require expensive operations, particularly for costly non-linear functions. These non-linear functions are computed via expensive high-degree polynomials (Lu et al., 2025; Pang et al., 2024). We notice that we can reduce the high-degree polynomials to their low-degree counterparts for the less important tokens. As demonstrated in Figure 7 (a), the cost of reduced polynomial can be $0.1\times$ that of the high-degree polynomial. This motivates us to accelerate the non-linear operations with low-degree polynomials while maintaining the desired accuracy. Similar to employing a threshold θ to prune tokens with importance scores below θ , we use another reduction threshold β ($\beta > \theta$) to identify tokens for reduction. As shown in Figure 7 (b)(c), combining token pruning with polynomial reduction further reduces execution time compared to the pruning-only method. Importantly, we can optimize both θ and β together during offline fine-tuning to enhance efficiency. During the online inference phase, polynomial reduction occurs after token pruning (the pruning ratio greater than zero). This simplifies the reduction process: the tokens have already been pruned, and the locations of these tokens are rotated and concealed. Consequently, there’s no need to safeguard the token mask for reduction. Instead, we can simply modify the pruning protocol Π_{Prune} to establish the reduction protocol. As illustrated in Figure 8, the pruned tokens are determined by executing protocols Π_{prune} and Π_{mask} in tandem. A secure comparison with the reduction threshold β then produces the reduction mask $\langle M_\beta \rangle$. The location of this mask corresponds to pruned tokens, not the original tokens, so revealing it does not compromise the location privacy of reduced tokens, provided that the privacy of pruned locations is maintained. Once the reduction mask M_β is known to each party, it can be used to guide the decision on whether to apply the high-degree polynomials or low-degree ones for the non-linear functions, where 1 indicates using the high-degree ones and 0 signifies low-degree ones. The choice of these approximation polynomials can be flexible. We utilize prior non-linear function approximation methods as detailed in references such as (Kim et al., 2021; Lu et al., 2025; Pang et al., 2024). The specific configurations used are outlined in the Appendix C.

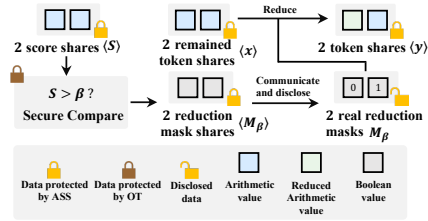


Figure 8: Secure polynomial reduction.

3.4 NETWORK OPTIMIZATION FOR ENCRYPTED PRUNING AND POLYNOMIAL REDUCTION

To support online token pruning and non-linear approximation, an offline fine-tuning method is needed to optimize pruning and approximation thresholds, θ and β , to minimize inference overhead and achieve user-defined accuracy above a . This process is challenging because (1) previous studies have not incorporated the efficiency and accuracy of encrypted token pruning and non-linear approximation into the fine-tuning phase, and (2) the thresholds for different Transformer layers vary and are challenging to pinpoint. To address these challenges, we introduce a crypto-aware fine-tuning method,

Algorithm 1 Crypto-aware Thresholds Learning

-
- Input: pre-trained Transformer \mathcal{M} , training data \mathcal{D} , initial thresholds θ, β
1. Set model \mathcal{M} with L layers, weights w , input tokens x , accuracy requirement a , and hyperparameters T, λ, α .
 2. Search for optimal thresholds θ, β and weights w on data \mathcal{D} .
 - (a) For $l \in [L]$, set soft masks for token x_i , $M_\theta^{(l)}(x_i) = \sigma(\frac{S^{(l)}(x_i) - \theta^{(l)}}{T})$ and $M_\beta^{(l)}(x_i) = \sigma(\frac{S^{(l)}(x_i) - \beta^{(l)}}{T})$.
 - (b) For $l \in [L]$, integrate the crypto-friendly polynomial activation functions. In the l -th layer, compute GELU function as: $\text{GELU}(x_i) = M_\beta^{(l)}(x_i) \cdot \text{GELU}(x_i) + (1 - M_\beta^{(l)}(x_i)) \cdot \text{ApproxGELU}(x_i)$. Except for the first layer, compute SoftMax function as: $\text{SoftMax}(x_i) = M_\beta^{(l-1)}(x_i) \cdot \text{SoftMax}(x_i) + (1 - M_\beta^{(l-1)}(x_i)) \cdot \text{ApproxSoftMax}(x_i)$. For the input feature x_{in} , compute the output feature x_{out} in the l -th layer as: $x_{out} = M_\theta^{(l)}(x_{in}) \cdot x_{out}$
 - (c) Update w, θ and β jointly to minimize the loss \mathcal{L} , where $\mathcal{L} = \mathcal{L}_{task} + \lambda(\mathcal{L}_{prune} + \alpha\mathcal{L}_{approx.})$.
 3. Finetune w on data \mathcal{D} with learned thresholds θ and β .
 - (a) Fix the threshold θ, β . Binarize the mask $M_\theta^{(l)}$ in every layer as:

$$M_\theta^{(l)}(x_i) = \begin{cases} 1 & \text{if } S^{(l)}(x_i) > \theta^{(l)}, \\ 0 & \text{otherwise.} \end{cases}$$
 , and $M_\beta^{(l)}$ is binarized in the same way.
 - (b) Update w to minimize the loss \mathcal{L}_{task} . Derive the optimal fine-tuned transformer \mathcal{M}^* .
 4. Output θ, β and w if accuracy $\geq a$; otherwise back to step 2.
-

outlined in Algorithm 1. This method uses a gradient search approach and proposes to incorporate crypto-aware pruning and approximation into the training phase. Additionally, the loss functions are designed to optimize both efficiency and accuracy.

After initialization, we make the masks differentiable during fine-tuning to allow for trainable thresholds, as shown in step 2.(a) of Algorithm 1. Here, T represents the temperature, and σ is the Sigmoid function. This soft mask, a differentiable approximation of the binary mask, enables gradient-based updates to θ and β . In step 2.(b) of the same algorithm, we introduce polynomial activation functions during the fine-tuning phase. ApproxSoftMax and ApproxGELU are low-degree polynomial approximations of the SoftMax and GELU functions. The ApproxSoftMax replaces the exponential function e^x in original SoftMax with a Taylor series $(1 + \frac{x}{2^n})^{2^n}$. And the ApproxGELU leverages simple polynomials such as $p^3(x) = -0.51 - 0.42x^2 + -0.12x^2 - 0.01x^3$ to approximate GELU. We defer the detailed polynomial in Equations 5 and 8 in the Appendix C. If a token x_i 's importance score exceeds the threshold β , it activates mainly through the original SoftMax or GELU functions; otherwise, through their polynomial approximations.

$$\mathcal{L}_{prune} = \frac{1}{L} \sum_{l=0}^{L-1} \|M_\theta^{(l)}(x)\|_1, \mathcal{L}_{approx.} = \frac{1}{L} \sum_{l=0}^{L-1} \|M_\beta^{(l)}(x)\|_1 \quad (3)$$

The overall objective function is designed to minimize the loss function $\mathcal{L} = \mathcal{L}_{task} + \lambda(\mathcal{L}_{prune} + \alpha\mathcal{L}_{approx.})$ where L denotes the number of layers. \mathcal{L}_{task} optimizes accuracy for downstream tasks, while \mathcal{L}_{prune} and $\mathcal{L}_{approx.}$, defined by M_θ 's and M_β 's l_1 -norms respectively, target efficiency as detailed in Equation 3. The hyperparameters λ and α dictate the extent of pruning and approximation, with higher values leading to increased pruning or approximation. This structure introduces additional gradients, pushing θ and β towards minimizing \mathcal{L}_{prune} and $\mathcal{L}_{approx.}$. Once the optimized θ and β are determined, we fix them and proceed to fine-tune the model weights to meet the accuracy requirement a as specified in Step 3. For each Transformer layer, we binarize the masks M_θ and M_β to select tokens for pruning or approximation. Subsequently, we update the model weights to minimize the downstream task loss \mathcal{L}_{task} .

4 EXPERIMENTS

4.1 EXPERIMENTAL SETUP

Models and Datasets. We evaluated CipherPrune on the GPT2-Base and three BERT variants (Devlin et al., 2018): BERT-Medium, BERT-Base, and BERT-Large. These models are commonly used in private Transformer frameworks. Similar to prior work (Pang et al., 2024), we fine-tune the BERT models on four downstream NLP tasks in GLUE benchmarks (Wang et al., 2018): the Multi-Genre Natural Language Inference Corpus (MNLI), the Stanford Question Answering Dataset (QNLI), the Stanford Sentiment Treebank (SST-2), and the Microsoft Research Paraphrase Corpus (MRPC).

System Setup and Implementation. We encode floating-point parameters in Transformers into fixed-point numbers and set the scale according to prior work (Hao et al., 2022; Lu et al., 2025; Pang et al., 2024). CipherPrune uses the EzPC (EzP, 2023) framework and the SEAL (SEA, 2023) library. EzPC compiles TensorFlow-based deep neural networks into secure computation protocols running on cryptographic backends. We simulate LAN with 3Gbps bandwidth and 0.8ms ping, and WAN with 200Mbps bandwidth and 40ms ping, following (Pang et al., 2024). All experiments are conducted on an AMD Ryzen Threadripper PRO 3955WX (2.2GHz, 125GB RAM) and fine-tuning of the BERT model with threshold learning is done on NVIDIA GeForce RTX 3090 GPUs with CUDA 11.0.3.

4.2 RESULTS

Table 1: End-to-end comparison of CipherPrune with prior works on BERT models. Time is in seconds. Comm. stands for communication in GB and Acc. for accuracy in percentage.

Method	BERT Medium			BERT Base			BERT Large		
	Time	Comm.	Acc.	Time	Comm.	Acc.	Time	Comm.	Acc.
IRON (Hao et al., 2022)	442.4	124.5	87.7 \pm 0.2	1087.8	281.0	90.4 \pm 0.1	2873.5	744.8	92.7 \pm 0.1
BOLT w/o W.E. (Pang et al., 2024)	197.1	27.9	87.4 \pm 0.3	484.5	59.6	90.3 \pm 0.1	1279.8	142.6	92.6 \pm 0.2
BOLT (Pang et al., 2024)	99.5	14.3	87.2 \pm 0.3	245.4	25.7	89.9 \pm 0.3	624.3	67.9	92.4 \pm 0.2
CipherPrune	43.6	6.7	87.4 \pm 0.2	79.1	9.7	90.1 \pm 0.2	157.6	18.4	92.5 \pm 0.1

End-to-end performance. In Table 1, we evaluate CipherPrune on three BERT models, comparing it with previous private Transformer frameworks: IRON (Hao et al., 2022) and BOLT (Pang et al., 2024). CipherPrune achieves up to $\sim 18.2\times$ speedup over IRON on the BERT-Large model and $\sim 8.1\times$ speedup over vanilla BOLT without W.E.. When compared with BOLT with the word elimination technique, CipherPrune is still $\sim 3.9\times$ faster without compromising accuracy. Communication costs are also reduced by $2.3 \sim 40.4\times$ compared to prior works. Compared with BOLT, CipherPrune can remove more redundant tokens during inference through the adaptive and progressive pruning strategy. Moreover, CipherPrune also leverages low-degree polynomials to further reduce the computation and communication overhead. CipherPrune can easily extend to other frameworks. Comparison with more related works like BumbleBee (Lu et al., 2025), MPCFormer (Li et al., 2022) and PUMA (Dong et al., 2023) can be found in Appendix D.

Table 2: Accuracy and time comparisons of different methods. CipherPrune[†] stands for CipherPrune with token pruning only.

Method	Accuracy Metric on Tasks (%)				Time(Sec)
	MNLI	QNLI	SST2	MPRC	
BOLT w/o W.E.	84.75	90.32	91.74	90.53	484.5
BOLT	84.71	89.94	92.74	89.95	245.4
CipherPrune [†]	84.74	90.17	92.75	90.45	115.3
CipherPrune	84.68	90.11	92.66	90.18	79.1

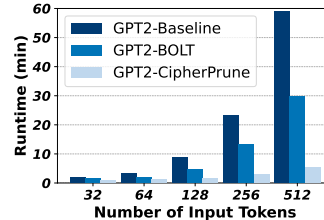


Figure 9: Runtime on GPT2.

Token pruning and polynomial reduction. Table 2 demonstrates the effects of the main design blocks in CipherPrune: adaptive token pruning and polynomial reduction. Our baseline is the vanilla BOLT framework without W.E.. BOLT’s W.E. removes 50% of the input tokens and effectively cuts the overhead of cryptographic protocols by half. With fine-tuning, the W.E. incurs only marginal accuracy loss. Yet, the adaptive and progressive token pruning in CipherPrune[†] can further improve the utility-accuracy trade-off. Instead of setting the pruning ratio as 50% manually, CipherPrune[†] adaptively decides the pruning ratio based on both the input length and content. This contributes to up to 0.5% better accuracy. On the other hand, the progressive pruning in CipherPrune[†] allows to remove more redundant information, contributing to $2.1\times$ runtime speed up over BOLT with W.E.. By incorporating polynomial reduction, CipherPrune can achieve up to $6.1\times$ speed up over BOLT. While the accuracy drops slightly from CipherPrune[†], it is still comparable or even higher than BOLT.

Scalability with the input length. In Figure 9, we compare the runtime of CipherPrune and BOLT with varying input token numbers on GPT2. The baseline is BOLT without W.E.. The quadratic complexity of Transformer inference makes it challenging for BOLT to scale to long inputs. Although W.E. can reduce the overhead of private inference by half, BOLT with W.E. still scales quadratically

with the number of input tokens. In contrast, CipherPrune demonstrates increasingly significant runtime savings as the input length grows. With 32 input tokens, CipherPrune achieves a $\sim 1.9\times$ speedup. When the input length reaches 512 tokens, CipherPrune is $\sim 10.6\times$ faster than the baseline.

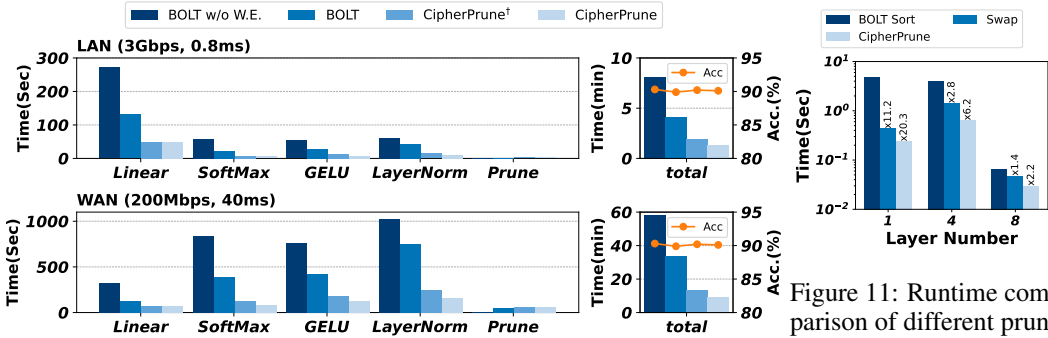


Figure 10: Runtime breakdown on BERT-Base model.

Figure 11: Runtime comparison of different pruning protocols.

Runtime breakdown. In Figure 10, we break down the runtime for each protocol in the BERT-Base model with 128 input tokens. In the LAN setting, the communication is efficient and the main bottleneck is the HE-based linear operation. In contrast, the massive communication of the non-linear operations becomes the bottleneck in the WAN setting. Since pruned tokens are excluded from the computation in all subsequent layers, CipherPrune can effectively reduce the overhead of both linear and non-linear operations. This contributes to CipherPrune’s efficiency in both LAN setting and WAN setting. As shown in Figure 10, the proposed pruning protocols in CipherPrune are lightweight, accounting for only 1.6% of the total runtime. This is because Π_{prune} leverages ASS to offload substantial computation to the local side, such as accumulating the importance score. Additionally, Π_{mask} utilizes the number of tokens in each layer to avoid sorting the whole token sequence.

Analysis on different pruning protocols. As shown in Figure 11, we compare the efficiency of different pruning protocols. BOLT’s W.E. uses Bitonic sort to sort the whole token sequence, which needs $O(n \log^2 n)$ oblivious swaps. In CipherPrune, the client and server only need $O(mn)$ oblivious swaps to relocate and prune the less important tokens. Since only a small number of tokens are removed in each layer, CipherPrune has a linear complexity to n in general. By binding the mask with tokens on the MSB, CipherPrune can handle the token sequence and pruning mask in one go and achieves $2.2 \sim 20.3\times$ speed up.

Study on the pruning parameters. In Figure 12, we show the accuracy-latency trade-off for the BERT-Base model under different parameter settings. Larger λ and α result in more tokens being pruned or reduced. With λ less than 0.05, an appropriate ratio of tokens is pruned, maintaining a stable accuracy of around 90%. Smaller α leads to more tokens being computed with high-degree polynomials, which increases accuracy but also latency. Notably, accuracy with a large α is higher than with a large λ . This is because many tokens are reduced but not discarded, preserving necessary information for accurate inference.

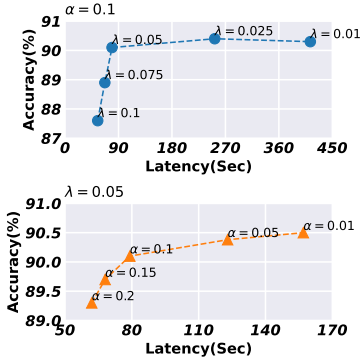


Figure 12: Ablation study on hyper-parameters λ and α .

5 CONCLUSION

The proposed CipherPrune addresses the critical efficiency and scalability challenges of private Transformer inference by introducing a novel approach that combines encrypted token pruning and polynomial reduction protocols. By progressively pruning redundant tokens and reducing the polynomial degree for less important tokens, CipherPrune significantly reduces runtime overhead while maintaining accuracy. Our experiments confirm its effectiveness, achieving a substantial reduction in execution time compared to previous methods.

REFERENCES

- 540
541
542 Ezpc. <https://github.com/mpc-msri/EzPC>, 2023.
- 543
544 Seal. <https://github.com/microsoft/SEAL>, 2023.
- 545 Gilad Asharov, Yehuda Lindell, Thomas Schneider, and Michael Zohner. More efficient oblivious
546 transfer and extensions for faster secure computation. In *Proceedings of the 2013 ACM SIGSAC*
547 *conference on Computer & communications security*, pp. 535–548, 2013.
- 548 Dan Bogdanov, Sven Laur, and Riivo Talviste. A practical analysis of oblivious sorting algorithms for
549 secure multi-party computation. In *Nordic Conference on Secure IT Systems*, pp. 59–74. Springer,
550 2014.
- 551 Zvika Brakerski. Fully homomorphic encryption without modulus switching from classical gapsvp.
552 In *CRYPTO*, volume 7417, pp. 868–886. Springer, 2012.
- 553 Tianyu Chen, Hangbo Bao, Shaohan Huang, Li Dong, Binxing Jiao, Daxin Jiang, Haoyi Zhou, Jianxin
554 Li, and Furu Wei. The-x: Privacy-preserving transformer inference with homomorphic encryption.
555 *arXiv preprint arXiv:2206.00216*, 2022.
- 556
557 Ronald Cramer, Ivan Bjerre Damgård, et al. *Secure multiparty computation*. Cambridge University
558 Press, 2015.
- 559
560 Jinming Cui, Chaochao Chen, Lingjuan Lyu, Carl Yang, and Wang Li. Exploiting data sparsity
561 in secure cross-platform social recommendation. *Advances in Neural Information Processing*
562 *Systems*, 34:10524–10534, 2021.
- 563 Jacob Devlin, Ming-Wei Chang, Kenton Lee, and Kristina Toutanova. Bert: Pre-training of deep
564 bidirectional transformers for language understanding. *arXiv preprint arXiv:1810.04805*, 2018.
- 565
566 Ye Dong, Wen-jie Lu, Yancheng Zheng, Haoqi Wu, Derun Zhao, Jin Tan, Zhicong Huang, Cheng
567 Hong, Tao Wei, and Wenguang Chen. Puma: Secure inference of llama-7b in five minutes. *arXiv*
568 *preprint arXiv:2307.12533*, 2023.
- 569 Junfeng Fan and Frederik Vercauteren. Somewhat practical fully homomorphic encryption. *IACR*
570 *Cryptol. ePrint Arch.*, pp. 144, 2012.
- 571
572 Qichen Fu, Minsik Cho, Thomas Merth, Sachin Mehta, Mohammad Rastegari, and Mahyar Na-
573 jibi. Lazyllm: Dynamic token pruning for efficient long context llm inference. *arXiv preprint*
574 *arXiv:2407.14057*, 2024.
- 575 Craig Gentry. *A fully homomorphic encryption scheme*. Stanford university, 2009.
- 576
577 Saurabh Goyal, Anamitra Roy Choudhury, Saurabh Raje, Venkatesan Chakaravarthy, Yogish Sab-
578 harwal, and Ashish Verma. Power-bert: Accelerating bert inference via progressive word-vector
579 elimination. In *International Conference on Machine Learning*, pp. 3690–3699. PMLR, 2020.
- 580 Meng Hao, Hongwei Li, Hanxiao Chen, Pengzhi Xing, Guowen Xu, and Tianwei Zhang. Iron: Private
581 inference on transformers. *Advances in Neural Information Processing Systems*, 35:15718–15731,
582 2022.
- 583
584 Xiaoyang Hou, Jian Liu, Jingyu Li, Yuhan Li, Wen-jie Lu, Cheng Hong, and Kui Ren. Ciphertgpt:
585 Secure two-party gpt inference. *Cryptology ePrint Archive*, 2023.
- 586
587 Zhicong Huang, Wen-jie Lu, Cheng Hong, and Jiansheng Ding. Cheetah: Lean and fast secure {two-
588 party} deep neural network inference. In *31st USENIX Security Symposium (USENIX Security 22)*,
pp. 809–826, 2022.
- 589 Gyuwan Kim and Kyunghyun Cho. Length-adaptive transformer: Train once with length drop, use
590 anytime with search. *arXiv preprint arXiv:2010.07003*, 2020.
- 591
592 Sehoon Kim, Amir Gholami, Zhewei Yao, Michael W Mahoney, and Kurt Keutzer. I-bert: Integer-
593 only bert quantization. In *International conference on machine learning*, pp. 5506–5518. PMLR,
2021.

- 594 Sehoon Kim, Sheng Shen, David Thorsley, Amir Gholami, Woosuk Kwon, Joseph Hassoun, and Kurt
595 Keutzer. Learned token pruning for transformers. In *ACM SIGKDD Conference on Knowledge*
596 *Discovery and Data Mining*, pp. 784–794, 2022.
- 597 Vladimir Kolesnikov and Ranjit Kumaresan. Improved ot extension for transferring short secrets. In
598 *Advances in Cryptology—CRYPTO 2013: 33rd Annual Cryptology Conference, Santa Barbara, CA,*
599 *USA, August 18–22, 2013. Proceedings, Part II*, pp. 54–70. Springer, 2013.
- 600 Dacheng Li, Rulin Shao, Hongyi Wang, Han Guo, Eric P Xing, and Hao Zhang. Mpcformer: fast,
601 performant and private transformer inference with mpc. *arXiv preprint arXiv:2211.01452*, 2022.
- 602 Wen-jie Lu, Zhicong Huang, Zhen Gu, Jingyu Li, Jian Liu, Cheng Hong, Kui Ren, Tao Wei, and
603 Wenguang Chen. BumbleBee: Secure Two-party Inference Framework for Large Transformers.
604 In *32nd Annual Network and Distributed System Security Symposium, NDSS 2025*. The Internet
605 Society, 2025.
- 606 Jinglong Luo, Yehong Zhang, Zhuo Zhang, Jiaqi Zhang, Xin Mu, Hui Wang, Yue Yu, and Zenglin
607 Xu. Secformer: Towards fast and accurate privacy-preserving inference for large language models.
608 *arXiv preprint arXiv:2401.00793*, 2024.
- 609 Qi Pang, Jinhao Zhu, Helen Möllering, Wenting Zheng, and Thomas Schneider. Bolt: Privacy-
610 preserving, accurate and efficient inference for transformers. In *2024 IEEE Symposium on Security*
611 *and Privacy (SP)*, pp. 4753–4771. IEEE, 2024.
- 612 Alec Radford, Karthik Narasimhan, Tim Salimans, Ilya Sutskever, et al. Improving language
613 understanding by generative pre-training. 2018.
- 614 Deevashwer Rathee, Mayank Rathee, Nishant Kumar, Nishanth Chandran, Divya Gupta, Aseem
615 Rastogi, and Rahul Sharma. Cryptflow2: Practical 2-party secure inference. In *Proceedings of the*
616 *2020 ACM SIGSAC Conference on Computer and Communications Security*, pp. 325–342, 2020.
- 617 Deevashwer Rathee, Mayank Rathee, Rahul Kranti Kiran Goli, Divya Gupta, Rahul Sharma, Nishanth
618 Chandran, and Aseem Rastogi. Sirnn: A math library for secure rnn inference. In *2021 IEEE*
619 *Symposium on Security and Privacy (SP)*, pp. 1003–1020. IEEE, 2021.
- 620 Ashish Vaswani, Noam Shazeer, Niki Parmar, Jakob Uszkoreit, Llion Jones, Aidan N Gomez, Łukasz
621 Kaiser, and Illia Polosukhin. Attention is all you need. *Advances in neural information processing*
622 *systems*, 30, 2017.
- 623 Alex Wang, Amanpreet Singh, Julian Michael, Felix Hill, Omer Levy, and Samuel R Bowman. Glue:
624 A multi-task benchmark and analysis platform for natural language understanding. *arXiv preprint*
625 *arXiv:1804.07461*, 2018.
- 626 Hanrui Wang, Zhekai Zhang, and Song Han. Spatten: Efficient sparse attention architecture with
627 cascade token and head pruning. In *IEEE International Symposium on High-Performance Computer*
628 *Architecture*, pp. 97–110. IEEE, 2021.
- 629 Tianshi Xu, Lemeng Wu, Runsheng Wang, and Meng Li. Privcirnet: Efficient private inference via
630 block circulant transformation. *arXiv preprint arXiv:2405.14569*, 2024.
- 631 Wenxuan Zeng, Meng Li, Wenjie Xiong, Tong Tong, Wen-jie Lu, Jin Tan, Runsheng Wang, and
632 Ru Huang. Mpcvit: Searching for accurate and efficient mpc-friendly vision transformer with
633 heterogeneous attention. In *IEEE/CVF International Conference on Computer Vision*, pp. 5052–
634 5063, 2023.
- 635 Jiawen Zhang, Xinpeng Yang, Lipeng He, Kejia Chen, Wen-jie Lu, Yinghao Wang, Xiaoyang
636 Hou, Jian Liu, Kui Ren, and Xiaohu Yang. Secure transformer inference made non-interactive.
637 *Cryptology ePrint Archive*, 2024.
- 638 Yuke Zhang, Dake Chen, Souvik Kundu, Chenghao Li, and Peter A Beerel. Sal-vit: Towards
639 latency efficient private inference on vit using selective attention search with a learnable softmax
640 approximation. In *IEEE/CVF International Conference on Computer Vision*, pp. 5116–5125, 2023.
- 641
- 642
- 643
- 644
- 645
- 646
- 647

Mengxin Zheng, Qian Lou, and Lei Jiang. Primer: Fast private transformer inference on encrypted data. In *IEEE/ACM Design Automation Conference, 2023*.

Itamar Zimerman, Moran Baruch, Nir Drucker, Gilad Ezov, Omri Soceanu, and Lior Wolf. Converting transformers to polynomial form for secure inference over homomorphic encryption. *arXiv preprint arXiv:2311.08610, 2023*.

APPENDIX

A SECURE TOKEN PRUNING PROTOCOLS

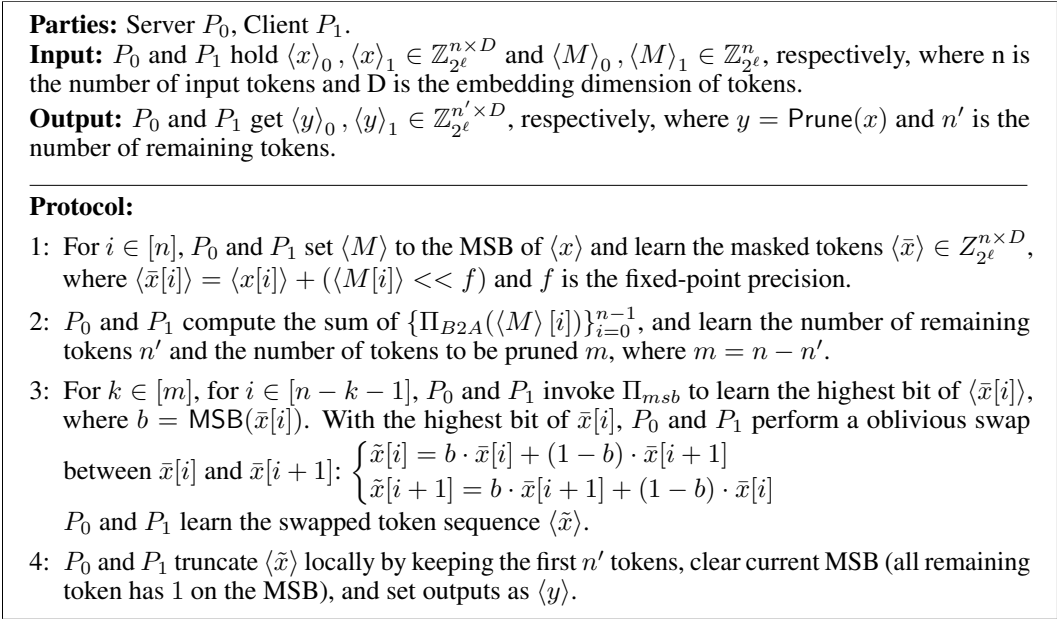
We detail the encrypted token pruning protocols Π_{prune} in Figure 13 and Π_{mask} in Figure 14 in this section.

<p>Parties: Server P_0, Client P_1.</p> <p>Input: P_0 and P_1 holds $\{\langle Att \rangle_0^h, \langle Att \rangle_1^h\}_{h=0}^{H-1} \in \mathbb{Z}_{2^\ell}^{n \times n}$ and $\langle x \rangle_0, \langle x \rangle_1 \in \mathbb{Z}_{2^\ell}^{n \times D}$ respectively, where H is the number of heads, n is the number of input tokens and D is the embedding dimension of tokens. Additionally, P_1 holds a threshold $\theta \in \mathbb{Z}_{2^\ell}$.</p> <p>Output: P_0 and P_1 get $\langle y \rangle_0, \langle y \rangle_1 \in \mathbb{Z}_{2^\ell}^{n' \times D}$, respectively, where $y = \text{Prune}(x)$ and n' is the number of remaining tokens.</p> <hr/> <p>Protocol:</p> <ol style="list-style-type: none"> 1: For $h \in [H]$, P_0 and P_1 compute locally with input $\langle Att \rangle^h$, and learn the importance score in each head $\langle s \rangle^h \in \mathbb{Z}_{2^\ell}^n$, where $\langle s \rangle^h[j] = \frac{1}{n} \sum_{i=0}^{n-1} \langle Att \rangle^h[i, j]$. 2: P_0 and P_1 compute locally with input $\{\langle s \rangle^i \in \mathbb{Z}_{2^\ell}^n\}_{i=0}^{H-1}$, and learn the final importance score $\langle S \rangle \in \mathbb{Z}_{2^\ell}^n$ for each token, where $\langle S \rangle[i] = \frac{1}{H} \sum_{h=0}^{H-1} \langle s \rangle^h[i]$. 3: For $i \in [n]$, P_0 and P_1 invoke Π_{CMP} with inputs $\langle S \rangle$ and θ, and learn $\langle M \rangle \in \mathbb{Z}_{2^\ell}^n$, such that $\langle M \rangle[i] = \Pi_{CMP}(\langle S \rangle[i] - \theta)$, where: $M[i] = \begin{cases} 1 & \text{if } S[i] > \theta, \\ 0 & \text{otherwise.} \end{cases}$ 4: P_0 and P_1 invoke Π_{mask} with inputs $\langle x \rangle$ and pruning mask $\langle M \rangle$, and set outputs as $\langle y \rangle$.

Figure 13: Secure Token Pruning Protocol Π_{prune} .

Complexity of Π_{mask} . The complexity of the proposed Π_{mask} mainly depends on the number of oblivious swaps. To prune m tokens out of n input tokens, $O(mn)$ swaps are needed. Since token pruning is performed progressively, only a small number of tokens are pruned at each layer, which makes Π_{mask} efficient during runtime. Specifically, for a BERT base model with 128 input tokens, the pruning protocol only takes $\sim 0.9s$ on average in each layer. An alternative approach is to invoke an oblivious sort algorithm (Bogdanov et al., 2014; Pang et al., 2024) on $\langle \bar{x} \rangle$. However, this approach is less efficient because it blindly sort the whole token sequence without considering m . That is, even if only 1 token needs to be pruned, $O(n \log^2 n) \sim O(n^2)$ oblivious swaps are needed, where as the proposed Π_{mask} only need $O(n)$ swaps. More generally, for an ℓ -layer Transformer with a total of m tokens pruned, the overall time complexity using the sort strategy would be $O(\ell n^2)$ while using the swap strategy remains an overall complexity of $O(mn)$. Specifically, using the sort strategy to prune tokens in one BERT Base model layer can take up to 3.8 \sim 4.5 s depending on the sorting algorithm used. In contrast, using the swap strategy only needs 0.5 s. Moreover, alternative to our MSB strategy, one can also swap the encrypted mask along with the encrypted token sequence. However, we find that this doubles the number of swaps needed, and thus is less efficient than our MSB strategy, as is shown in Figure 11.

702
703
704
705
706
707
708
709
710
711
712
713
714
715
716
717
718
719
720
721
722
723
724
725
726
727
728
729
730
731
732
733
734
735
736
737
738
739
740
741
742
743
744
745
746
747
748
749
750
751
752
753
754
755

Figure 14: Secure Mask Protocol Π_{mask} .

B EXISTING PROTOCOLS

Existing Protocols Used in Our Private Inference. In our private inference framework, we reuse several existing cryptographic protocols for basic computations. Π_{MatMul} (Pang et al., 2024) processes two ASS matrices and outputs their product in SS form. For non-linear computations, protocols $\Pi_{SoftMax}$, Π_{GELU} , and $\Pi_{LayerNorm}$ (Lu et al., 2025; Pang et al., 2024) take a secret shared tensor and return the result of non-linear functions in ASS. Basic protocols from (Rathee et al., 2020; 2021) are also utilized. Π_{CMP} (EzP, 2023), for example, inputs ASS values and outputs a secret shared comparison result, while Π_{B2A} (EzP, 2023) converts secret shared Boolean values into their corresponding arithmetic values.

C POLYNOMIAL REDUCTION FOR NON-LINEAR FUNCTIONS

The SoftMax and GELU functions can be approximated with polynomials. High-degree polynomials (Lu et al., 2025; Pang et al., 2024) can achieve the same accuracy as the LUT-based methods Hao et al. (2022). While these polynomial approximations are more efficient than look-up tables, they can still incur considerable overheads. Reducing the high-degree polynomials to the low-degree ones for the less important tokens can improve efficiency without compromising accuracy. The SoftMax function is applied to each row of an attention map. If a token is to be reduced, the corresponding row will be computed using the low-degree polynomial approximations. Otherwise, the corresponding row will be computed accurately via a high-degree one. That is if $M'_\beta[i] = 1$, P_0 and P_1 use high-degree polynomials to compute the SoftMax function on token $x[i]$:

$$\text{SoftMax}_i(x) = \frac{e^{x_i}}{\sum_{j \in [d]} e^{x_j}} \quad (4)$$

where x is a input vector of length d and the exponential function is computed via a polynomial approximation. For the SoftMax protocol, we adopt a similar strategy as (Kim et al., 2021; Hao et al., 2022), where we evaluate on the normalized inputs $\text{SoftMax}(x - \max_{i \in [d]} x_i)$. Different from (Hao et al., 2022), we did not use the binary tree to find max value in the given vector. Instead, we traverse through the vector to find the max value. This is because each attention map is computed independently and the binary tree cannot be re-used. If $M_\beta[i] = 0$, P_0 and P_1 will approximate the SoftMax function with low-degree polynomial approximations. We detail how SoftMax can be

approximated as follows:

$$\text{ApproxSoftMax}_i(x) = \frac{\text{ApproxExp}(x_i)}{\sum_{j \in [d]} \text{ApproxExp}(x_j)} \quad (5)$$

$$\text{ApproxExp}(x) = \begin{cases} 0 & \text{if } x \leq T \\ (1 + \frac{x}{2^n})^{2^n} & \text{if } x \in [T, 0] \end{cases} \quad (6)$$

where the 2^n -degree Taylor series is used to approximate the exponential function and T is the clipping boundary. The value n and T determines the accuracy of above approximation. With $n = 6$ and $T = -13$, the approximation can achieve an average error within 2^{-10} (Lu et al., 2025). For low-degree polynomial approximation, $n = 3$ is used in the Taylor series.

Similarly, P_0 or P_1 can decide whether or not to approximate the GELU function for each token. If $M_\beta[i] = 1$, P_0 and P_1 use high-degree polynomials (Lu et al., 2025) to compute the GELU function on token $x[i]$ with high-degree polynomial:

$$\text{ApproxGELU}(x) = \begin{cases} 0 & \text{if } x \leq -5 \\ P^3(x), & \text{if } -5 < x \leq -1.97 \\ P^6(x), & \text{if } -1.97 < x \leq 3 \\ x, & \text{if } x > 3 \end{cases} \quad (7)$$

where $P^3(x)$ and $P^6(x)$ are degree-3 and degree-6 polynomials respectively. The detailed coefficient for the polynomial is:

$$P^3(x) = -0.50540312 - 0.42226581x - 0.11807613x^2 - 0.01103413x^3$$

, and

$$P^6(x) = 0.00852632 + 0.5x + 0.36032927x^2 - 0.03768820x^4 + 0.00180675x^6$$

For BOLT baseline, we use another high-degree polynomial to compute the GELU function.

$$\text{ApproxGELU}(x) = \begin{cases} 0 & \text{if } x < -2.7 \\ P^4(x), & \text{if } |x| \leq 2.7 \\ x, & \text{if } x > 2.7 \end{cases} \quad (8)$$

We use the same coefficients for $P^4(x)$ as BOLT (Pang et al., 2024).

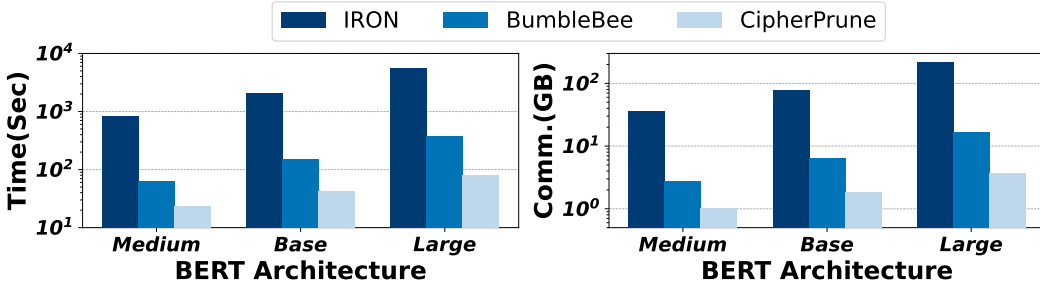


Figure 15: Comparison with prior works on the BERT model. The input has 128 tokens.

If $M'_\beta[i] = 0$, P_0 and P_1 will use low-degree polynomial approximation to compute the GELU function instead. Encrypted polynomial reduction leverages low-degree polynomials to compute non-linear functions for less important tokens. For the GELU function, the following degree-2 polynomial Kim et al. (2021) is used:

$$\text{ApproxGELU}(x) = \begin{cases} 0 & \text{if } x < -1.7626 \\ 0.5x + 0.28367x^2, & \text{if } x \in [-1.7626, 1.7626] \\ x, & \text{if } x > 1.7626 \end{cases}$$

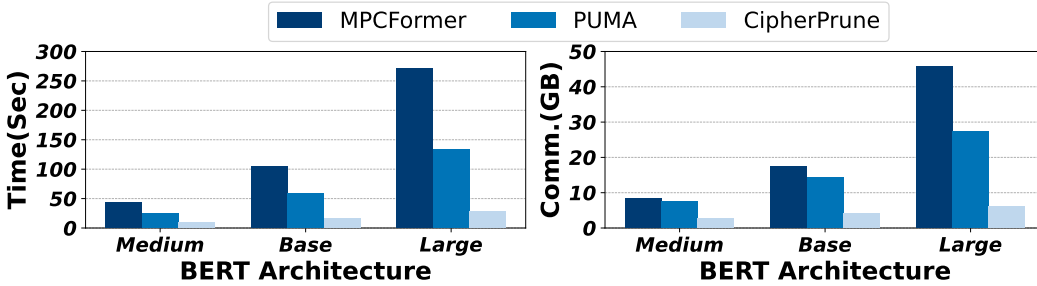


Figure 16: Comparison with MPCFormer and PUMA on the BERT models. The input has 128 tokens.

D COMPARISON WITH MORE RELATED WORKS.

Other 2PC frameworks. The primary focus of CipherPrune is to accelerate the private Transformer inference in the 2PC setting. As shown in Figure 15, CipherPrune can be easily extended to other 2PC private inference frameworks like BumbleBee (Lu et al., 2025). We compare CipherPrune with BumbleBee and IRON on BERT models. We test the performance in the same LAN setting as BumbleBee with 1 Gbps bandwidth and 0.5 ms of ping time. CipherPrune achieves more than $\sim 60\times$ speed up over BOLT and $4.3\times$ speed up over BumbleBee.

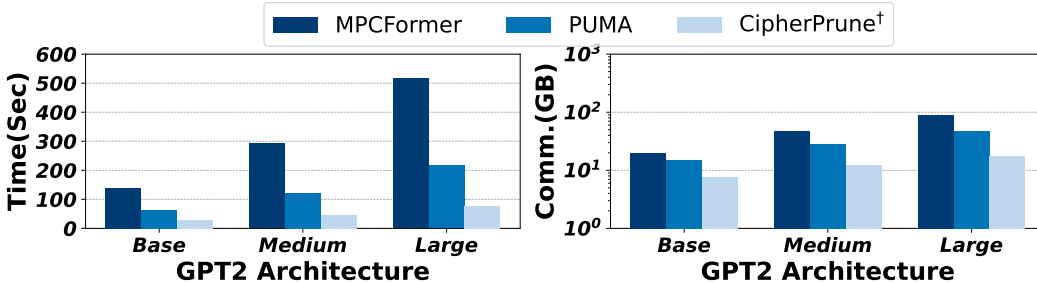


Figure 17: Comparison with MPCFormer and PUMA on the GPT2 models. The input has 128 tokens. The polynomial reduction is not used.

Extension to 3PC frameworks. Additionally, we highlight that CipherPrune can be also extended to the 3PC frameworks like MPCFormer (Li et al., 2022) and PUMA (Dong et al., 2023). This is because CipherPrune is built upon basic primitives like comparison and Boolean-to-Arithmetic conversion. We compare CipherPrune with MPCFormer and PUMA on both the BERT and GPT2 models. CipherPrune has a $6.6 \sim 9.4\times$ speed up over MPCFormer and $2.8 \sim 4.6\times$ speed up over PUMA on the BERT-Large and GPT2-Large models.

E COMMUNICATION REDUCTION IN SOFTMAX AND GELU.

In Figure 18, we illustrate why CipherPrune can reduce the communication overhead of both SoftMax and GELU. Suppose there are n tokens in $layer_i$. Then, the SoftMax protocol in the attention module has a complexity of $O(n^2)$. CipherPrune’s token pruning protocol is invoked to select n' tokens out of all n tokens, where $m = n - n'$ is the number of tokens that are removed. The overhead of the GELU function in $layer_i$, i.e., the current layer, has only $O(n')$ complexity (which should be $O(n)$ without token pruning). The complexity of the SoftMax function in $layer_{i+1}$, i.e., the following layer, is reduced to $O(n'^2)$ (which should be $O(n^2)$ without token pruning). The SoftMax protocol has quadratic complexity with respect to the token number and the GELU protocol has linear complexity. Therefore, CipherPrune can reduce the overhead of both the GELU protocols and the SoftMax protocol by reducing the number of tokens.

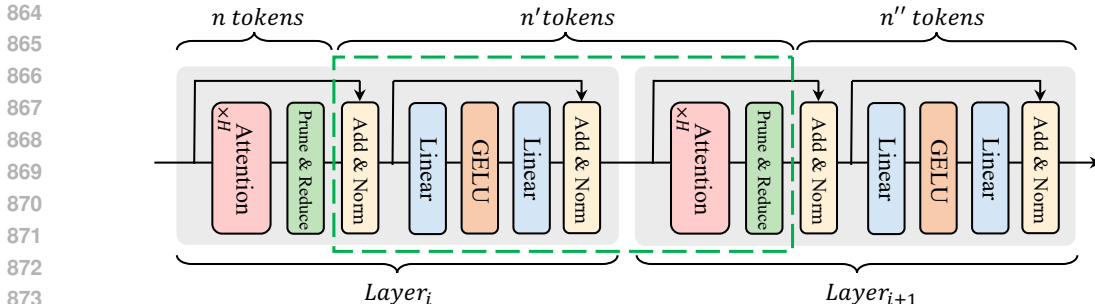


Figure 18: Toy example of two successive Transformer layers. In layer_{*i*}, the SoftMax and Prune protocol have *n* input tokens. The number of input tokens is reduced to *n'* for the Linear layers, LayerNorm and GELU in layer_{*i*} and SoftMax in layer_{*i*+1}.

F ANALYSIS ON LAYER-WISE REDUNDANCY.

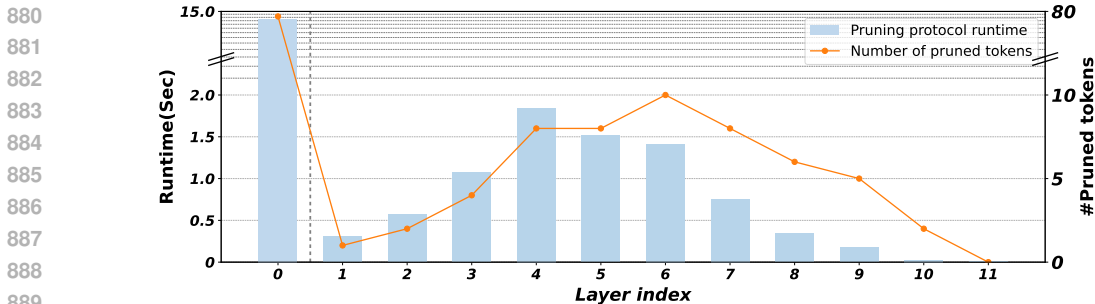


Figure 19: The number of pruned tokens and pruning protocol runtime in different layers in the BERT Base model. The results are averaged across 128 QNLI samples.

In Figure 19, we present the number of pruned tokens and the runtime of the pruning protocol for each layer in the BERT Base model. The number of pruned tokens per layer was averaged across 128 QNLI samples, while the pruning protocol runtime was measured over 10 independent runs. The mean token count for the QNLI samples is 48.5. During inference with BERT Base, input sequences with fewer tokens are padded to 128 tokens using padding tokens. Consistent with prior token pruning methods in plaintext (Goyal et al., 2020), a significant number of padding tokens are removed at layer 0. At layer 0, the number of pruned tokens is primarily influenced by the number of padding tokens rather than token-level redundancy.

In CipherPrune, tokens are removed progressively, and once removed, they are excluded from computations in subsequent layers. Consequently, token pruning in earlier layers affects computations in later layers, whereas token pruning in later layers does not impact earlier layers. As a result, even if layers 4 and 7 remove the same number of tokens, layer 7 processes fewer tokens overall, as illustrated in Figure 19. Specifically, 8 tokens are removed in both layer 4 and layer 7, but the runtime of the pruning protocol in layer 4 is $\sim 2.4\times$ longer than that in layer 7.

G RELATED WORKS

In response to the success of Transformers and the need to safeguard data privacy, various private Transformer Inferences (Chen et al., 2022; Zheng et al., 2023; Hao et al., 2022; Li et al., 2022; Lu et al., 2025; Luo et al., 2024; Pang et al., 2024) are proposed. To efficiently run private Transformer inferences, multiple cryptographic primitives are used in a popular hybrid HE/MPC method IRON (Hao et al., 2022), i.e., in a Transformer, HE and SS are used for linear layers, and SS and OT are adopted for nonlinear layers. IRON and BumbleBee (Lu et al., 2025) focus on optimizing linear general matrix multiplications; SecFormer Luo et al. (2024) improves the non-linear operations like the exponential function with polynomial approximation; BOLT (Pang et al., 2024) introduces the baby-step giant-step (BSGS) algorithm to reduce the number of HE rotations, proposes a word elimi-

918 nation (W.E.) technique, and uses polynomial approximation for non-linear operations, ultimately
919 achieving state-of-the-art (SOTA) performance.

920
921 Other than above hybrid HE/MPC methods, there are also works exploring privacy-preserving
922 Transformer inference using only HE (Zimmerman et al., 2023; Zhang et al., 2024). The first HE-
923 based private Transformer inference work (Zimmerman et al., 2023) replaces SoftMax function with
924 a scaled-ReLU function. Since the scaled-ReLU function can be approximated with low-degree
925 polynomials more easily, it can be computed more efficiently using only HE operations. A range-loss
926 term is needed during training to reduce the polynomial degree while maintaining high accuracy.
927 A training-free HE-based private Transformer inference was proposed (Zhang et al., 2024), where
928 non-linear operations are approximated by high-degree polynomials. The HE-based methods need
929 frequent bootstrapping, especially when using high-degree polynomials, thus often incurring higher
930 overhead than the hybrid HE/MPC methods in practice.

931
932
933
934
935
936
937
938
939
940
941
942
943
944
945
946
947
948
949
950
951
952
953
954
955
956
957
958
959
960
961
962
963
964
965
966
967
968
969
970
971